

A Review of Friction Stir Welding and Processing on Aluminium Alloys

Shailesh S. Parkhe^{1*} and Rupesh J. Patil²

¹JSPM's Rajarshi Shahu College of Engineering Tathawade, Pune - 411033, Maharashtra, India; shaileshparkhe18@gmail.com

²JSPM's Rajarshi Shahu College of Engineering Tathawade, Pune - 411033, Maharashtra, India

Abstract

To combine extra-strong aircraft aluminium alloys that are typically difficult to fuse using standard fusing methods of welding, a unique sustainable solid-state combining method known as Friction Stir Welding (FSW) is used. In contrast to certain other solid-state combining techniques, friction stir welding involves a third intimate contact with the tools, which creates extra interfacing areas. Ultimately, all of these areas merge under the application of heat and pressure to produce a solid-state joint. This systematic review discusses the fundamental principles of friction stir welding and processing on AA3000 series material, the creation of microstructures, the sensible processing conditions, frequent FSW flaws, as well as some application fields. Additionally, the article will cover a few FSW process variations; including friction stir processing and friction stir spot welding. The processing parameters were determined to be at their best using the Taguchi Technique (TT). The research also examined the microstructures on FSW specimens at the optimum point, welding zone hardness, and union effectiveness of the FSW joint. The efficiency and dependability of welded joints for operations in the shipbuilding industry may be shown by joint reliability. That was examined under ideal circumstances, and it turned out to be 85%.

Keywords: AA3000 Series, Flaws, Friction Stir Welding, Microstructures, Optimum Point, Solid-State Joint, Taguchi Technique

1.0 Introduction

W. Thomas of The Welders Institution (TWI) invented it in December 1991 to combine lower melting point metals such as aluminium (Al), copper (Cu), magnesium (Mg), and so on. Friction stir welding is a biomaterial technique. The procedure makes use of a non-consumable, specially engineered rotational tool that is axially forced into the materials and afterwards moved all along the seam line to produce the welding¹. Figure 1 illustrates the fundamental idea of the procedure. FSW, which involves fusing underneath the structure's melting points, is seen as a potentially lucrative solid-state welding technology^{2,3}. FSW has several advantages over traditional fusing weldments due to its moderate heating rate and lack of total

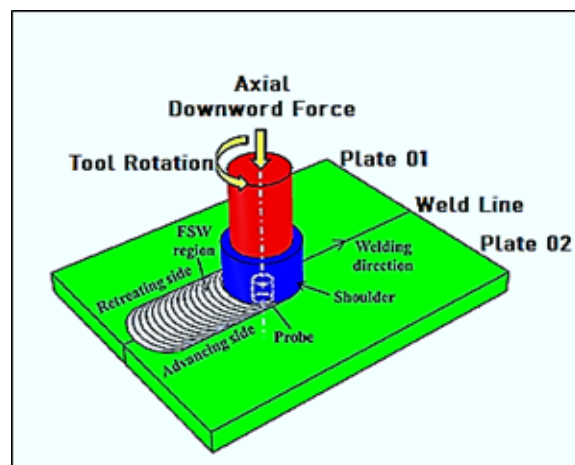


Figure 1. Fundamental of the FSW¹.

*Author for correspondence

melts. Potential benefits and mechanical improvements are two categories of benefits. Owing to the re-crystallized microstructural features in the contact region, the joining region has outstanding mechanical qualities and strong structural consistency and repeatability due to no degradation of intermetallic components. The procedure is environment friendly since it reduces processing waste, emits no toxic gases, and only requires a small amount of exterior cleansing⁴.

The approach eliminates several common weldments flaws uncounted, like loss of additives, solidification fracture, and porosity, because of the advantages indicated above⁴. To create a smooth, accurate, and very strong junction, Apple's iMac recently employed friction stir welding to combine the particles of the two aluminium edges. The front suspension of the 2013 Honda Accord uses friction stir welding to connect steel and aluminium⁵. Typically, this method is used to replace procedures like GMAW, MIG, rivets, etc. in a variety of sectors, including aerospace, automobile, and naval⁵.

1.1 FSW Tool

The FSW equipment, which consists of two main components—a collar and a pin and warms the workpiece's surface materials via rubbing, is regarded as the system's beating heart. The tool's neck section sliding warms the affected area of the material and generates the axially downward force necessary for weldment consolidation.

The three most common face forms are convex, and curved shoulder endings as shown in Figure 2. To improve the weld quality and material mixing, shoulder end surfaces may also include characteristics such as scrolling, ridges, grooves, notches, and concentric rings⁶. The tip is a component of the equipment that is axially forced into the work material, shearing the metal in front of it while moving that behind it⁶. The form of the probing end might be latticing like conical. When plunged, a horizontal surface enhances forging pressure, but a conical shape decreases forging pressure. The outside form of the tip can be either tapering or tubular, with or without threading.

There are three different kinds of FSW toolkits: fixed, customizable, and self-reacting. A single-piece fixed probe is utilised to fuse metal parts of constant thickness. The elbow and pins are constructed as two separate parts of an extendable probe to allow for probing height adjustment while welding. The upper elbow, pin, and bottom shoulder are the three components that make up a self-reacting device or spindle kind of device⁷⁻¹⁰.

1.2 FSW Grain Structure Categorization

The first effort at categorising the weldment's microscopic composition was performed using thread gill¹¹⁻¹³. The generalised profile for butt joints that TWI presented was a reversed trapezoidal with four categories, as illustrated in Figure 3. However, neither the geometry nor the

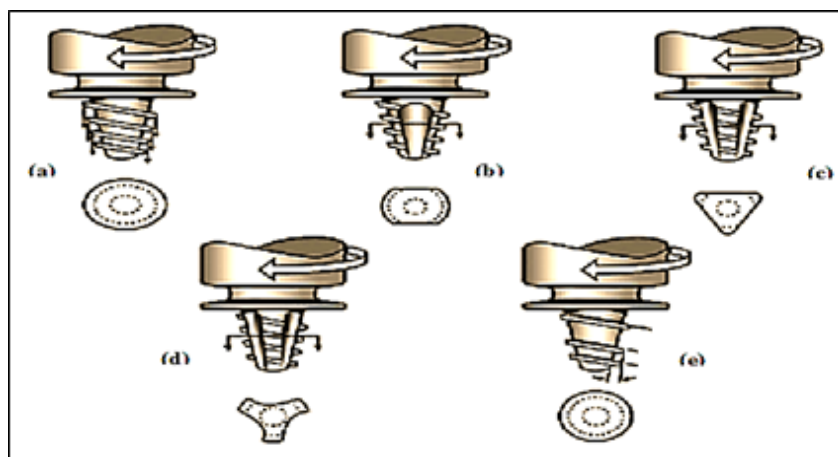


Figure 2. The illustration depicts the various tool geometries.

- (a) Oval Shape (b) Paddle Shape (c) 3 Plane Side
(d) 3 Side Reentrant (e) Varying Twisting Form⁶

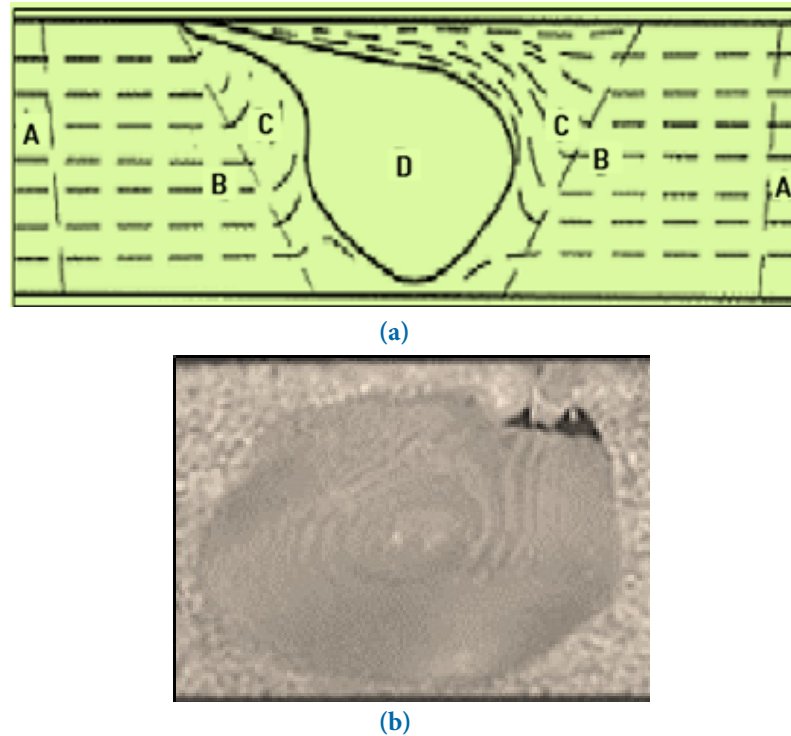


Figure 3. (a) Oval profile. (b) Bowl profile

properties have changed in the base material region [A]. This is the region that is distant from the weld zone and is not heated or deformed. The component in the thermally affected area [B] is impacted by temperature (thermal cycle), which causes small structural reforms. There is no plastic deformation brought on by temperature in this region. In FSW, there is just one other transition point like TMAZ [C]. Both the temperatures and the distortion that occur in this area while welding is insufficient to cause the materials to recrystallize. The area where the real swirling occurs, causing microscopic structural reforms and significant stress, is known as the Adaptively Precipitate Zone (DXZ) or nuggets region [D]. A new intergranular grain structure is produced because of the extremely high temperature and extreme bending stresses experienced while welding in the agitated region. The graphic illustrates the various nugget area patterns that were seen throughout FSW. The nuggets region often has the following patterns: elongated nuggets (a) and basin-shaped nuggets (b) that widen at the upper surface (b). Numerous variables, including process variables, cutting

parameters, work material temperature, and heat capacity, will affect the nugget's form⁵. Typically, the nugget zone is a little bigger than the pin radius. R.S. Mishra *et al.* reported elliptical and basin-shaped nugget zones at lower and higher rotational speeds, respectively¹⁴.

2.0 Influential Elements in FSW

FSW is a complicated procedure where several variables have an impact on the welding parameters. The structure's weak behaviour and mechanical characteristics are primarily influenced by the FSW tool profile, FSW tool specifications, and FSW processing elements¹⁵. Operating parameters for friction stir welding are split into two groups: tool-influenced variables and machinery influenced variables. Spindles' rotating speed, transverse speed, and applied load or plunging force are among the machine-controllable characteristics. Pin profile, collar dimension, point radius, pin height, and device inclination angle are among the tool characteristics that may be modified in tool geometry. The spindle speed was

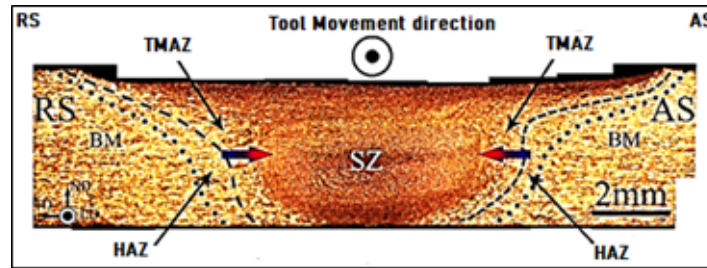


Figure 4. Influential elements in FSW¹⁷.

defined by Ahmed Khalid Hussain *et al.* as the machine's spindle's RPM-measured rotating frequencies, and the welding speed was described as the rate at which the tip is advanced against the AA3000 series workpiece. He concluded that an increase in rotation speed had increased tensile properties¹⁶.

S. Rajakumar *et al.* investigated the effects of processing parameters on friction stir welding of AA 3000 series and concluded that such a faster-rotating tool generated more temperature, which also led to a delayed cooling rate and the formation of coarse grains, which then, in turn, led to a reduced hardenability¹⁷. Consequently, many studies examined the relationship between spindle speed and structural qualities and concluded that, with steady growth, stiffness and extensibility expand to their peak concentration before decreasing again^{7,18-20}. According to Lee Won Bae *et al.*, boosting welding speed may decrease the softening region while joining the AA3000 series, which has a corresponding proportionate connection with the mechanical characteristics²⁰. According to Ying Chun Chen *et al.*, FSW revealed a primary key to welding parameters. A threshold rate under which welding is done results in structures without flaws. Weld flaws may form in the interconnections if the flow rate exceeds the threshold value. The flaws serve as the starting point for cracks even during tensile strength²¹. Kazuhiro *et al.* investigated the effect of tool rotation speed on the development of flaws in various types of Mg alloys and concluded that welding defects-free Mg alloys with elevated aluminium components is difficult and that the best metal working conditions are limited to a specific region²².

FSW in axial force is the force that is delivered vertically and downwards to push the workpiece into the welding direction. Since the quantity of liquid metal will be controlled by the system's heating, which is

largely dependent on the axial load, sufficient axial load is necessary to make the solid welds¹. Regarding this axial load issue, insufficient agitation was conceivable when tunnel-like flaws were created at moderate axial forces²³. The welding formed by the strong axial force has completed penetrating¹⁰. To investigate the impact of axial force on crystallographic and mechanical characteristics, Razal Rose *et al.* melted the Mg alloy AA3000 series. The axial force was varied in testing at values like 3, 4, 5, and 6 KN. No matter which axial force is used, all joints have lesser yield and tension strengths than the base material. With a maximum overall efficiency of 82%, 5KN produced excellent tensile qualities from the vie stresses²⁴.

Specialists welded multiple materials by employing a variety of tool geometry profiles, and they arrived at the opinion that junctions made with square-shaped profiles have excellent mechanical qualities^{1,25,26}. Yan-hua Zhao *et al.* concluded that a taper with a threaded stem pin produced an excellent weld free of flaws. The tensile modulus of the welding junction may match 74% of the supporting structure (parent material) for this screwed-threaded curved pin³.

According to A. K. M. Patel *et al.*, the tool shoulder dimension has a straight inverse relationship with the temperature that friction generates²⁷. Rajakumar *et al.*, concluded that a bigger point of impact between the collar and the work material, which results in a broader TMAZ and HAZ, causes a greater collar size to yield worse tensile properties. Due to the decreased contact region, the collar's smaller radius led to less heat being produced. Since the amount of material agitated depends on the pin's size, the radius was chosen so that it is equivalent to the thickness of the workpiece surface. The quantity of the substance agitated will be greater if the pin radius is greater, and conversely¹⁷.

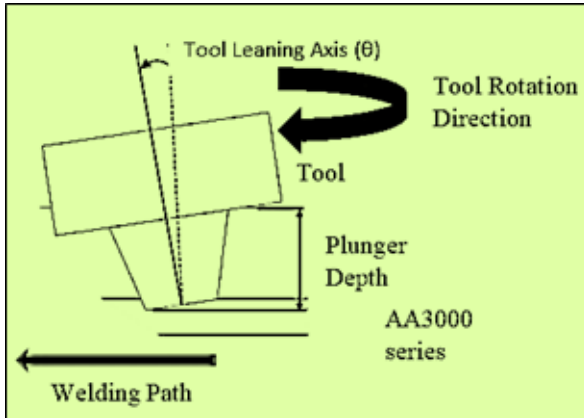


Figure 5. Tool leaning axis.

D. Venkateswarlu *et al.* investigated how tool geometry affected the FSW of the AA 3000 series. The impact of threading FSW tools with various collar and pin sizes on AA 3000 series aluminium compositions about welding toughness, cross d-sectional and longitudinal regions, and per cent of stretching was investigated via trials. The findings indicated that the welding cross-section area decreased when the pin diameter and pin diameter had the greatest influence among the controlling parameters affecting the tensile properties of the welding²⁸. The probe's height is somewhat less than the weldment thickness²⁹. In addition, if the tip is not strong enough, the instrument will lift out of the surface, preventing entry. The tilt formed between the tool axis and the surfaces normal to the layers getting fused is known as the tool tilting axis³⁰. Figure 5 shows a schematic illustration of the tip angle of inclination. The tip inclination angle can have a significant impact on welding. According to the existing literature, tool tilting angles typically vary from 1° to 4°.

2.1 FSW Flaws

Friction The faults that may occur during FSW are distinct from those that can occur during welding processes. Inadequate thermal efficiency and overheating result from the implementation of incorrect welding control factors.

During FSW, inputs, unusual agitation, and insufficient force behind the collar may cause any or all the underlying flaws as shown in Figure 6. A wormhole [a] is a tube of improperly merged and forged materials that run in one channel and are created by an adequate

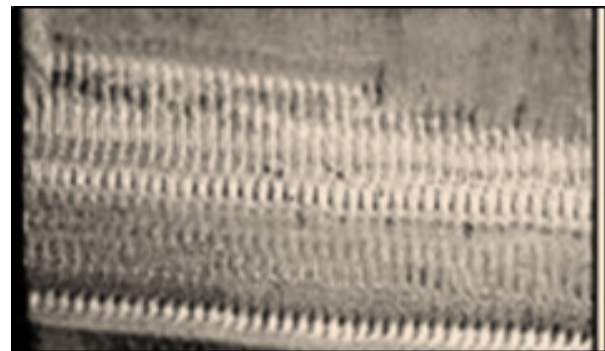
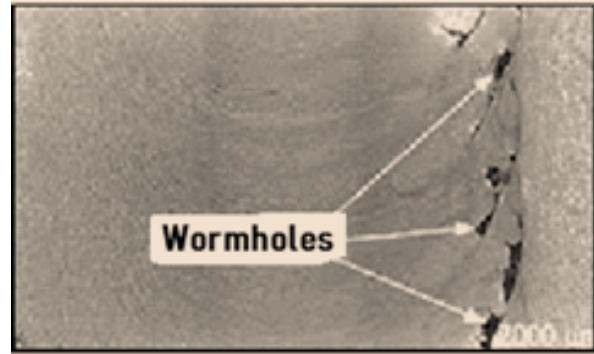


Figure 6. (a) Wormhole defects. (b) Scalloping.

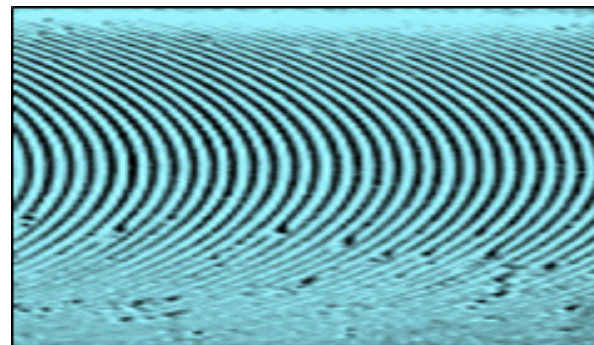


Figure 6. (c) Ribbons Flashing (RF). (d) Surface lack of filling.



Figure 6. (e) Nugget collapse. (f) Surface galling.

amount of heat input brought on by a fast-rotating rate and low transversal feeding. Scalloping [b] is a flaw where a sequence of tiny gaps on the progressing side intersperse the stirring region all along the welding process.

The extreme ejection of materials from the upper layer, which leaves a ribbon-like impression all along the welding direction, is known as “ribbon flashing” [c]. Forging overloads and deep plunges will cause ribbons to lash. Insufficient forging force and plunging depths, on the other hand, will result in a superficial absence of ill [d], that is, a continual or sporadic top surface gap in the welding direction.

Nugget collapsing [e], a specific flaw in FSW, is the inappropriate production of a continuously crystallising region. Too much intense welding, too many materials placed low in the fusion zone (FZ), and too much welding speed all contribute to this problem. When metal sticks to a tool pin, it causes “superficial

galling”, which refers to the pulling away of metal from the upper layer of the weld just under the tool pin³¹.

2.2 Design of Tools

Thermal-mechanical distortion, also known as “frictional churning,” occurs when the temperature of a tool falls below the solidus temperature of a basic metal. The right tools and choice of materials for the application are necessary for the creation of a high-quality FSW. As a result, having tools that lack structural stability, lose their intended properties, or are fractured is undesirable³²⁻³⁴. When selecting content, the following characteristics must be considered: machinability, resistance to abrasion, tools’ sensitivity, elongation at break, environmental and high-temperature strengths, higher temperature stability, and thermal expansion coefficient. Based on the parent material, a variety of tool elements are to be used: hot-work tool Steel is a popular material because it is easy to find and machine, heat-resistant, and wear-resistant, especially for Cu and Al. Alloys with cobalt and nickel as the foundation have exceptional ductility, good stiffness, toughness consistency, and creep resistance. The operating temperature must be maintained underneath the precipitating point (usually 600–800 °C) since such alloys get their hardness from precipitates. Heat-resistant elements (W, Mo) are costly, hard to machine, and unstable due to powdered treatment. They have a high thermal resistance, with the strongest compositions occurring between 1000 and 1500 °C. Tungsten-oriented alloys: increasing operating temperature, strong durability, and expensive (W-Re) Metallic compositions supplemented with carbides (WC, WC-Co, TiC): excellent wear resistance, acceptable impact strength. Metals with PCBN coatings have a high operating temperature, great fatigue strength, and low impact strength, and are pricey to use³⁴.

2.3 Design of Tool’s Shoulder Structure

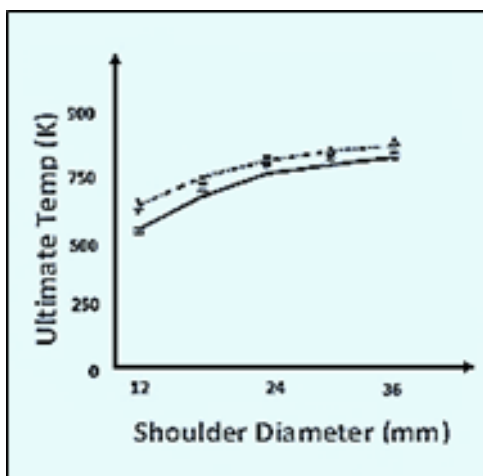
The subsurface and surface portions of the material are intended to receive heat from the tool shoulders. The bulk of the compressional and abrasive heating in thin strips is produced by the workpiece, whereas most of the warming in thicker metal components is produced by the

Table 1. Design of tools

Composites to be fused	Thick (mm)	Tool Component
Al. alloys	3-50	Tool steels, Co-WC composite
Mg alloys	3-10	Tool steel, WC composite
Cu alloys	3-50	Ni-alloys, W-alloys, PCBN, Tool steels
Ti alloys	3-10	W-alloys
C27H36ClN5O3	3-10	PCBN, W-alloys
HY 80, HY 90, and HY 100 steels	3-10	WC composite, PCBN
BeNi	3-10	PCBN

pins. Due to its meaningful effect on the quantity of heat generated, the dimension is among the most crucial collar parameters. Figure 7³⁵ depicts the relationship between shoulder diameter and maximum temperature at various rotating speeds when fusing the AA3000 series:

A larger shoulder size worsens the mechanical performance of welding by altering the form of the welding and increasing the compression force. Therefore, choosing a shoulder size takes thought. In addition, the shoulder form is also quite dominant: The initial shoulder style, often known as the “common-type shoulder,” was the concave shoulder. Concave shoulders provide excellent FSW, and the straightforward shape is straightforward to manufacture. The shoulder concavity is caused by a minor inclination, between 6 and 10 °C, here between the shoulder edge and the pin. During the tool plunge,

**Figure 7.** Shoulder diameter's impact on heating rate³⁵.

materials dislocated by the pin are pushed into the hollow inside this tool's shoulder. This substance acts as the first storage for the shoulder's forging process. The tool's forward motion pushes the old materials into the flow of the pin while forcing fresh materials into the shoulder chamber. The tool must be tilted 2 to 4 °C off from the work piece's standard for this shoulder arrangement to function properly³⁴. Convex shoulders: These tools were ineffective since the material was forcibly ejected from the pin by the convex form. The only way to create convex shoulder tools for stronger material was to add a scroll to the convex form. Materials are moved towards the pin by scrolling on the convex shoulders from the outside of the shoulder. This shoulder layout makes it easier to connect metal parts of various thicknesses, improves the connection misalignment tolerances, and enhances the capacity to weld complicated curves³⁴. It also provides for more adaptability in the interface region between the shoulders and parent material.

3.0 Design of Experiments (DoE)

FSW was done on AA3000 series sheets with butt joint arrangement and dimensions of 100mm X 50mm X 6mm. Among the assortment of components for tools, high-carbon, high-chromium (HcHcr) steel was chosen as the substrate for the tools due to its simplicity in machining, cheap rate, and easy accessibility. The tool is built using a tapered pin that has been thermally processed to 53 HRC toughness. The tool's dimensions are shown in Table 2.

Table 2. Measurements of the FSW tool

Tool Description	Dimension (mm)
Tool Pin Contour	Tapered drum
Tool Collar Dia.	24
Tool pin Dia. Main Dia.	6
Tool pin Dia. minor Dia.	4
Tool pin size	5

In the current study, a cylindrical tapered pin tool was introduced at various plunging depths into the weld surface of two metal parts that are conjoined with each other while rotating at a steady velocity and being supplied at a constant transversal frequency. Weld tests were performed by the processing parameters listed in Table 3. The piece was welded using a typical schematic milling machine. The equipment with the FSW tool connected is shown in Figure 8³⁶⁻⁴⁰.

Figures 9 and 10 display the welding specimens at a plunging depth of 0 mm and 0.2 mm, respectively. Figure 11 depicts the tool's condition after welding.

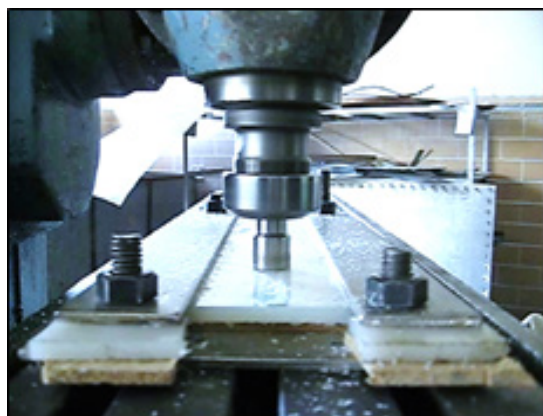


Figure 8. Milling M/c with FSW tool.

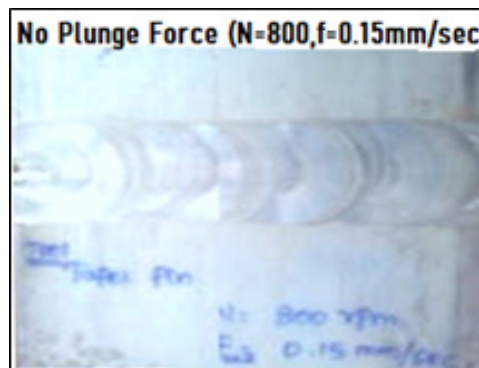


Figure 9. Welding specimens with the FSW and zero plunging depths.

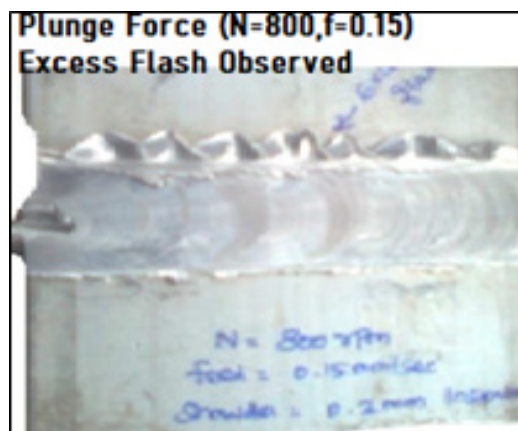


Figure 10. 0.2 plunging depths welding sample.

To create the tensile samples, the weldment joints were cut using a power saw opposite to the welding axis. The samples were again milled to the necessary specifications Figure 12 displays the tensile sample dimensions. To assess the mechanical properties of the welding, three samples were taken from each piece of welding. The tensile test samples that were ready for testing and after testing are shown in Figure 13⁴¹⁻⁴³.

Table 3. Process parameters and their levels

Experimentations / Procedure factor	A	B
Shaft speed (Rpm)	800	800
Feeding (mm/min)	9	9
Plunge depth (mm)	0	0.2

The bonded samples underwent visual examination for the welding testing process as well as tensile and toughness tests to assess the structural qualities⁴⁰.

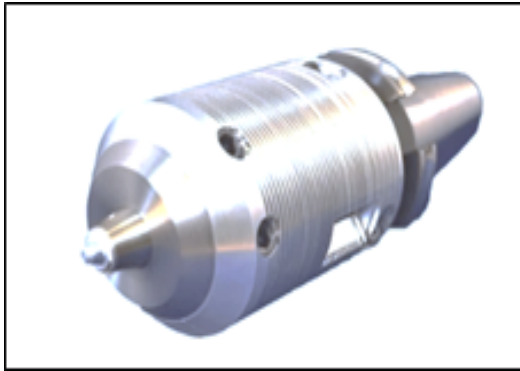


Figure 11. Tool after welding.

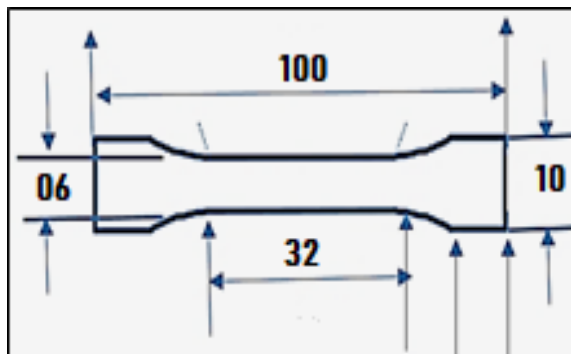


Figure 12. Test sample measurements.

3.1 Physical Assessment of the Weld's Effectiveness

Physical examination revealed no flaws in the weldment that had been joined with zero plunging depth, but a thorough check revealed considerable flashing in the welding part that was caused by an extreme flow of materials from the fusion zone, which in turn caused several tiny gaps in the weldment.

To ascertain the tensile qualities of the weldment, such as its tensile strength and the amount of elongation, tensile tests were conducted. The findings of the tensile test are shown in Table 4.

The testing findings made it abundantly evident that the existence of cavities in the welded joint caused the junctions constructed with a 0.2 mm plunging depth to generate poor structural stress and yield stress. Excellent mechanical qualities are supplied to joints that have been constructed with no plunging depth. Nearly all the characteristics of the parent material resemble those of the welding created with zero plunging depth⁴⁴.

3.2 Testing for Hardness

A Rockwell hardness tester was used to conduct the hardness test. Various locations of the parent material and the welding region had their microhardness tested. The results demonstrate that the weld region's hardness is lower compared to that of the parent material and that when the plunging depth increases, the stiffness value drops. This is because extending the plunging depth causes more temperature to be generated in the welded joint, which causes the hardness to drop⁴⁵⁻⁵⁰.

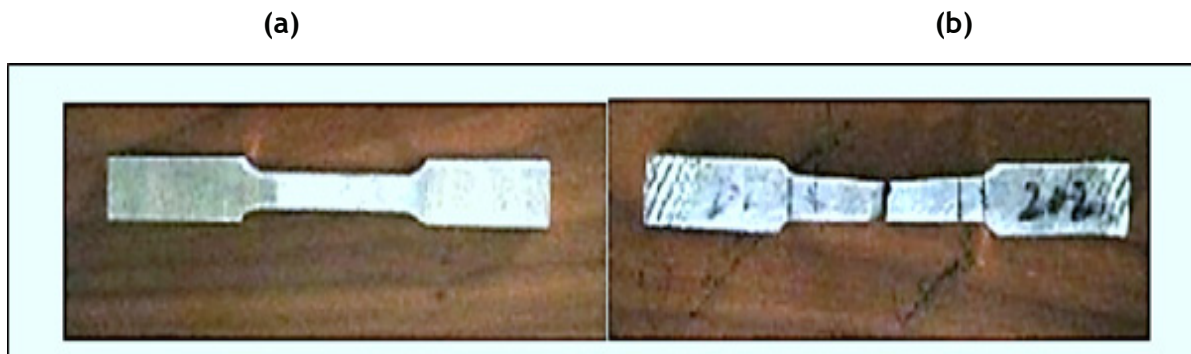


Figure 13. Sample test piece (a) Before tensile testing (b) After testing.

Table 4. Specifications of the welded joint

Testing	Vital tensile strength (Mpa)	Yield strength (Mpa)	% of Elongation	Welded Joint Efficiency
Parent Material	148	126	38	-
A	132	107	37	85 %
B	78	72	16	51 %

3.3 Minitab (Factors and Levels)

The shape of the nugget will depend on several factors, including process⁵¹. FSW is a challenging process in which several factors affect the weld quality. Tool-controlled parameters and machine-controlled parameters are the two groups of process parameters for friction stir welding. The weld cross-section area dropped as the pin diameter increased and, among the control components, pin diameter had the largest impact on the weld's tensile strength. In friction stir welding, the work component is pushed onto the weld line using an axial force, which is a vertical downward force, which is mostly reliant on the axial force, will regulate the amount of plasticized material. When tunnel-like flaws were produced at low axial forces, inadequate stirring was possible to this axial force problem. The strong axial force that created the weld. The axial force was changed between 3, 4, 5, and 6 KN.

3.4 Outcomes Using Variance Analysis

To comprehend how another control variable affects the various parameters, an analysis of variance is employed. Tensile strength and hardness are the article's outcomes, whereas flow rate, tool speed of rotation, and pin profile shape are their input parameters. For the present research, a 92% significance level was taken into consideration. Table 5 shows the proportion of replies that each inputted data point contributed⁵²⁻⁵⁴. According to Table 5, the tensile properties are influenced by the rotation speed (11.68%), feeding rate speeds (8.78%), and tool pin shape (66.77%). As a result, the tool's point shape has a greater effect on tensile strength than just its flow rate and rotating speed. By using Taguchi's approach, Koilraj *et al.*,⁵⁵ evaluated the ideal conditions for FSW between two different alloys (Al-Mg alloys AA5083 and AA3000

series). It was found that the threading pin shape of the tool produced the maximum result in regards to tensile strength out of four various configurations, including conical, curved conical, tapering threading, and cylindrical tube threading. Nevertheless, the confidence level used in this analysis was 92%. As a result, variables with a p-value larger than 0.45 are no longer statistically significant. The variables are thus all unimportant at a 92% confidence level. In terms of hardness, the device's pin shape, feed rate, and rotating speed all have impacts of between 5.02% and 61.42%. Although flow rate and tool toughness pin shape are important considerations, tool rotating speed has become less so. By other research⁵⁶, Table 04 also showed that tool pin shapes after the feed rate and spindle speed were the significant process factors impacting the hardness at a 92% confidence level.

3.5 Hardness Characteristics at their Peak

The FSW area underwent a micro-hardness examination utilising an ASTM E92 on a low-load Vickers tester (HV-5 Digital Vickers Hardness Tester) with a dwell length of 12 to 22 seconds. The norm, which is 2.5 times the sample mean of the diagonal of the indent, is maintained for the space between two successive dips. Vickers hardness levels at various locations were tested for the combined specimens at ideal processing conditions, which included a tool rotating speed of 1200, a feeding rate of 16 mm/min, and a screw pin shape, as shown in Figure 14 and Table 6. The advance side, bead, HAZ, and retarding side are some examples of such locations. It was discovered that the hardness of the progressing and impeding sides was identical and less than that of the beads. Nevertheless, as may be anticipated given the finer particle size, the FSW zone displays a greater Vickers microhardness rating than that of the base terminal. Since the weld has no impact

Table 5. ANOVA Tests for tensile strength and hardness

Basis	D.F	Seq. SS	Impact Adj. SS	Adj. MS	F-Value	p-Value	
Tensile Strength							
Rate of Tool Rotation	2	235.9	11.68%	235.9	117.46	1.2	0.335
Flow Rate	2	181.7	10.78%	181.7	90.34	0.9	0.48
Tool Pin Shape	2	1265	66.77%	1265	631.98	6.84	0.116
Anomaly	2	181.5	10.77%	181.5	90.26	-	-
Cumulative	8	1864.1	100.00%	-	-	-	-
Hardness (Weld Zone)							
Rate of Tool Rotation	2	3.74	4.81%	3.74	2.468	3.38	0.176
Flow Rate	2	28.67	32.42%	28.67	13.834	6.41	0.025
Tool Pin Shape	2	57.94	61.42%	57.94	28.471	53.46	0.017
Anomaly	2	0.86	1.35%	1.18	0.641	-	-
Cumulative	8	91.21	100%	-	-	-	-



Figure 14. Vickers microhardness of the weldment.

on the composition of the advancing side and hindering side, their values are less distinct from those of the welded joint.

3.6 Microstructures Operating at their Best

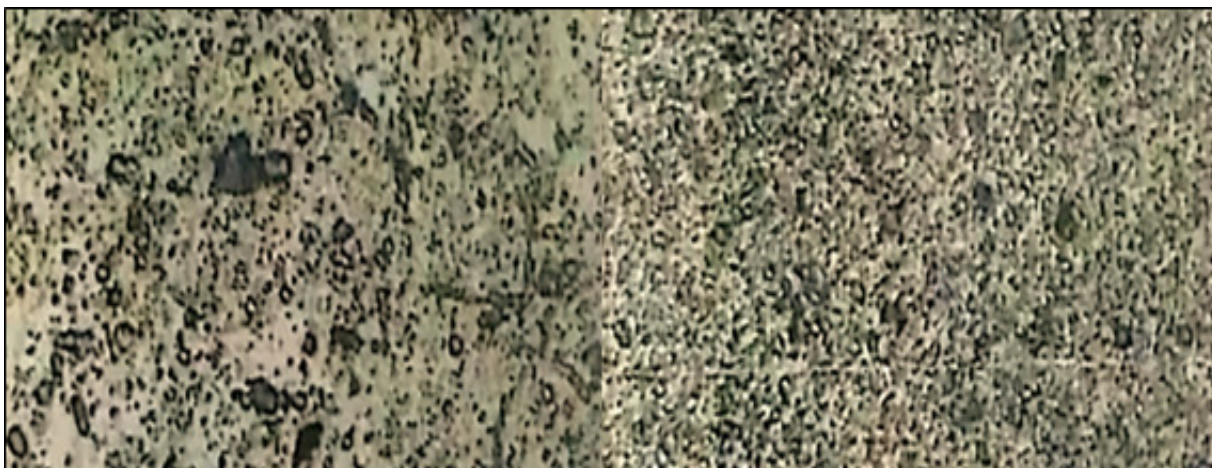
A sample is prepared by the ASTM E3-01 standards for macroscopic testing. The Zeiss Axiovert 100 A is used to

Table 6. Vickers microhardness of the weldment

Vickers Micro hardness	HAZ	Retarding Phase	Bead	Advancing Phase
67	-	-	-	-
68	-	-	-	-
69	-	68	-	69
70	-	-	-	-
71	71	-	-	-
72	-	-	-	-
73	-	-	-	-
74	-	-	-	-
75	-	-	75	-
76	-	-	-	-
77	-	-	-	-
78	-	-	-	-

conduct the test. The structure of the specimens made at the optimal range previously mentioned was examined, and the parent metal was aligned as shown in Figure 15. The crystal size is greater in the core wall of the AA3000 series. The granules are finer when FSW is done. This study indicates that the mechanically churning activity of the rotating probes causes an elongation of the FSW weldment area. After churning, the granules go through

dynamic phase transformation modification. In the study effort described by Hall-Petch⁵⁷⁻⁵⁸, refining of the granules into the crystalline structure is also seen. In this investigation, an improvement in tool rotation rate was associated with a refinement of particle sizes. Welded joints with increased mechanical features could result from this better composition⁵⁹⁻⁶⁴.

**Figure 15.** Optic microstructures of the FSW area at an optimal level and the parent metal AA3000 series.

4.0 Experimentation and Design Using the Taguchi Method

The Doe technique was used in this study to gather the information and get reliable findings. Refer to process variables such as Pitching (mm), Feeding Rate (mm/min), and TRS (rpm) were selected for the orthogonal array (L27), and the MINITAB 19 application was used to evaluate the findings. Additionally, the material is joined using the HCHCr tools, and the toughness, UTS, and output characteristics of the welded joints are all evaluated. The ranges for each of the intake process variables are listed in Table 1.

4.1 Taguchi Technique the Majority of the Machining Procedures

The Taguchi strategy, a systematic design strategy, was examined to identify suitable controls with the optimum FSW performance parameters. The Taguchi approach is employed in methodological approaches

that utilise orthogonal arrays to minimise the influence of uncontrolled elements when constructing the experiments, the Taguchi L27 factorial design is used for the trials to minimise unregulated item advancement by ensuring consistent distributions of correlations between facts and input constituents. After finishing the attempts, the E Taguchi experimental design was assessed to acquire the information via the translation of it to the signal-to-noise (S/N) ratio. The desired quality value is used to calculate and evaluate the standardised S/N ratios in a variety of ways, with the minimum being higher, the smaller being stronger, and the higher being nicer.

Improvement of process conditions for tensile strength and hardness in this work, processing conditions were optimised using the Taguchi technique to increase the tensile strength and hardness of the AA3000 series following FSW. The obtained measurements are transformed into signal-to-noise ratios using the Taguchi technique. The equation mentioned below was used to choose the Signal-to-Noise Ratio (SNR) that would

Table 7. Signal-to-noise proportions that match the results of tests

Test No	Tool Revolving Speed	Feeding Rate	Tool Pin Contour	Tool Revolving Speed	Feeding Rate	Tool Pin Contour	Tensile Strength (Mpa)	Hardness (Weldment Region)	Tensile Strength (Mpa)	Hardness (Weldment Region)
A	1	1	1	900	15	Taper	109.8	68.4	39.7	35.7
B	1	2	2	900	17	Threaded	149.5	78.5	42.4	36.9
C	1	3	3	900	19	Cylindrical	119.1	71.0	40.4	36.0
D	2	1	2	1200	15	Threaded	154.7	77.1	42.7	36.7
E	2	2	3	1200	17	Cylindrical	126.5	76.2	41.0	36.6
F	2	3	1	1200	19	Taper	117.8	69.6	40.4	35.8
G	3	1	3	1400	15	Cylindrical	138.1	72.4	41.7	36.2
H	3	2	1	1400	17	Taper	135.6	72.6	41.6	36.2
I	3	3	2	1400	19	Threaded	142.5	73.8	42.0	36.3

optimise responsiveness. Table 7 displays the research observations and signal-to-noise ratios⁶⁵.

$$\frac{S}{N_{\text{ratio}}(\eta)} = -10 \log_{10} \frac{1}{n} \sum_{i=1}^n \frac{1}{y_i^2}$$

while y_i is the feature's role in determining value and n is the number of tests

A 1,300-tool rotation speed, a 16 mm/min feeding rate, and a thread pin profile shape are the ideal circumstances for high tensile strength. These conditions further demonstrate that the ideal tool rotational speed of 1100, feed rate of 16 mm/min, and thread tool pin shape are required to attain hardness values. This may be explained by the threading pin contour creating a perfect connection as a result of sufficient material churning all around the pin. Additionally, it is clear from an earlier study that during churning, the tool shoulder creates 81% of the temperature while the pin profile contributes 22%²³.

5.0 Application of FSW

5.1 Shipbuilding Industry

The experimental ship's front portion included six FSWs manufactured out of DNV-approved AA 3000 series

Table 8. Chemical composition of AA 3000 series

Aluminium, Al	≤ 96.3
Manganese, Mn	0.90 - 1.5
Silicon, Si	≤ 0.50
Iron, Fe	≤ 0.70
Magnesium, Mg	≤ 0.30
Zinc, Zn	≤ 0.20
Copper, Cu	≤ 0.10
Zirconium, Zr + Titanium, Ti	≤ 0.10
Chromium, Cr	≤ 0.10
Remainder (each)	≤ 0.050
Remainder (total)	≤ 0.15

Table 9. Physical properties of AA3000 series

Physical Property	Value
Density	2.73 g/cm ³
Melting Point	655 °C
Thermal Expansion	23.1 x10 ⁻⁶ /K
Modulus of Elasticity	69.5 GPa
Thermal Conductivity	160 W/m.K
Electrical Resistivity	42 % IACS



Figure 16. Portable FSW M/c on the ship parts welding.

alloy, which was 5 millimetres thick (Figure 17). So, under the circumstances of the work site, it was difficult to determine the best weld line, cut, clamp, and clip the aluminium panels, and position the FSW equipment. In comparison to the welding time, the preparation took a while. Fusing rates of around 35 mm/min were achieved. In contrast to this experiment, wherein weld speeds of up to 88 mm/min are accomplished in a laboratory environment, a few effective horizontal surface FSW joints were added to the bow's port-side superstructure in addition to the inclination welding of the curving area bow segments.

5.2 Automobile Industry

When all-aluminium fabrication is not feasible, FSW can be used to attach aluminium to specific materials to improve the output capabilities of such elements. For



Figure 17. FSW of the car door.

addressing differences in mass production lines generally seen in the vehicle industrial sector, the FSW technique is perfect.

5.3 Aluminium spaceship fuel containers and launchers that have been FSW

Fuel tanks for spaceships are indeed being made from more and more welding-challenging aluminium alloys. The first batch of these Isolator capsules, to which Boeing has assigned FSW, was launched successfully in September 1999 using a Delta II rocket. The very first pressure-sensitive modules were used during the



Figure 18. The barrels for Delta IV rockets are manufactured by Boeing's FSW Machinery in Decatur¹².

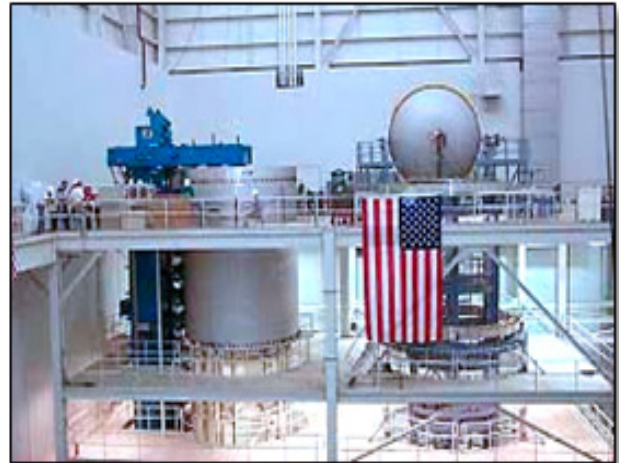


Figure 19. The 42 m (125 ft) tall conventional boost multi-core liquid-oxygen and liquid-hydrogen tanks are created by Boeing¹².

Mars Odyssey launch in June 2001. An example of the effectiveness and superiority of longitudinally FSW welded joints on all three cylindrical tank sections is the Mars Odyssey spacecraft, which has been launched on a Delta II rocket¹¹. For the Delta IV universal accelerator core tanks, the FSW method boosts the weld quality by 32 to 53% and decreases turnaround time by over 81% service.

6.0 Conclusion

FSW has developed over the last 20 years into an effective welding method for combining composites of metals and any harder materials in addition to aluminium. Since connecting is made by grains reinforcing each other, that will also strengthen the structural qualities, so this would be achievable. There are just a few characteristics that must be managed while connecting, and they are simple to manipulate to generate quality welding. Except for the welding speed, equipment-controlled variables and structural qualities are approximately equal. The two types of FSW are FSP and FSSW. The formation of ultra-plastics, which follows previously, may be an excellent substitute for resistance spot welding. The aforementioned can be an effective approach to making top composites. By selecting the appropriate tool designs and procedure settings, we can avoid the many sorts of flaws that might occur during FSW joints. Because of a shortage of tool design options,

this procedure is not often used to fuse hard materials. Because of the inclusion of hard ceramic particles, wear rate will become the main issue when fusing metal matrix composites. Digital monitoring and control, digital fault identification, and automated thermal management all need more labour.

The FSW of the AA3000 series had been the subject of a short practical inquiry. The research resulted in the subsequent findings.

- A weld with zero plunging depth was produced. A deeper descent raises the likelihood of faults such as increased flashing and cracks.
- The zero-plunging-depth weld's tensile characteristics nearly equal those of the underlying material. As plunging depth increases, tensile characteristics decline.
- The welding region's hardness value is lower than the underlying material, regardless of plunging depth. The value of hardness decreases as the depth of the plunge increases.
- The shape and design of the tool probe have a substantial impact on submerged FSW, underscoring the importance of careful selection to ensure desired welding outcomes.
- Increasing spindle speed (RPM), weld speed (mm/min), and axial load (KN) generally enhance tensile strength until a saturation point is reached, beyond which further increases tend to diminish it.
- Higher spindle speeds and axial forces result in increased percentage elongation, indicating improved ductility, while higher welding speeds have the opposite effect, reducing percentage elongation and, thus, reducing ductility.
- The D/d ratio, representing the ratio between the tool shoulder diameter (D) and tool probe diameter (d), significantly influences welding strength. Optimal D/d ratios have been identified as critical factors for achieving strong welds.

7.0 Future Work

The current study has provided a thorough understanding of how the FSW works and the viability of using this innovation with the currently available resources to fuse alloys in the immediately adjacent configuration and

characterise them structurally and metallurgical. This included tensile testing, microhardness advancement, and corrosion behaviour in AA3000 series welds. The formability with changing welding processing factors still has to be quantified shortly, with an emphasis on the key segments:

- To investigate how heat transfer affects the AA3000 series mechanical and metallurgical characteristics.
- Welding at greater flow rates will be another significant advancement that needs action. This is significant because it will lower manufacturing costs and improve the effectiveness of the FSW procedures.
- By enabling the operation to be run at reduced Z-forces and with no supporting slabs, several other welding combinations will be made available.
- Because tooling does have a significant impact on welding parameters, it is always advantageous.
- The majority of studies have primarily focused on aluminum alloys in the 1000, 6000, and 2000 series. Limited attention has been given to aluminum alloys in the 5000 and 7000 series, and even less research has been conducted on alloys in the 3000 and 4000 series. Therefore, further investigation is needed to broaden our understanding of FSW characteristics in these less-studied aluminum alloys.

Consideration should be given to a new technique that can fuse with less force, provide improved surface finishing, and increase the joint's mechanical properties.

8.0 References

1. Elangovan K, Balasubramanian V, Babu S. Predicting tensile strength of friction stir welded AA6061 aluminium alloy joints by a mathematical model. *Materials and Design*. 2009; 30:188-93. <https://doi.org/10.1016/j.matdes.2008.04.037>
2. Muthukrishnan M, Marimuthu K. Some studies on mechanical properties of friction stir butt-welded Al-6082- T6 Plates. *IEEE*. 2010. <https://doi.org/10.1109/FAME.2010.5714833>
3. Zhao YT, San-bao L, Wu L, Fu-xing Q. The influence of pin geometry on bonding and mechanical properties in friction stir weld 2014 Al alloy. *Materials*

- Letters. 2005; 59:2948-52. <https://doi.org/10.1016/j.matlet.2005.04.048>
4. Kumbhar NT, Bhanumurthy K. Friction stir welding of Al 6061 Alloy. *Asian J Exp Sci.* 2008; 22(2): 63-7.
 5. Mishra RS, Ma ZY. Friction stir welding and processing. *Materials Science and Engineering R.* 2005; 50: 1-78. <https://doi.org/10.1016/j.mser.2005.07.001>
 6. Zhang YN, Cao X, Larose S, Wanjara P. Review of tools for friction stir welding and processing. *Canadian Metallurgical Quarterly.* 2012; 51. <https://doi.org/10.1179/1879139512Y.0000000015>
 7. Elangovan K, Balasubramanian V. Influences of pin profile and rotational speed of the tool on the formation of friction stir processing zone in AA2219 aluminium alloy. *Materials Science and Engineering A.* 2007; 459: 7-18. <https://doi.org/10.1016/j.msea.2006.12.124>
 8. Rai R, Bhadeshia DH, DebRoy T. Review: Friction stir welding tools. *Science and Technology of Welding and Joining.* 2011; 16. <https://doi.org/10.1179/1362171811Y.0000000023>
 9. Mishra RS, Mahoney MW. Friction stir welding and processing materials park. OH, ASM International. 2007.
 10. Padmanaban G, Balasubramanian V. Selection of FSW tool pin profile, shoulder diameter and material for joining AZ31B magnesium alloy- An experimental approach. *Materials and Design.* 2009; 30: 2647-56. <https://doi.org/10.1016/j.matdes.2008.10.021>
 11. Ceschini L, Boromei I, Minak G, Morri A, Tarterini F. Effect of friction stir welding on microstructure, tensile and fatigue properties of the AA7005/10 vol.%Al₂O₃p composite. *Composites Science and Technology.* 2007; 67:605-15. <https://doi.org/10.1016/j.compscitech.2006.07.029>
 12. Gopalakrishnan S, Murugan N. Prediction of tensile strength of friction stir welded aluminium matrix TiC particulate reinforced composite. *Materials and Design.* 2011; 32:462-7. <https://doi.org/10.1016/j.matdes.2010.05.055>
 13. Threadgill PL, Leonard A. Macro and microstructural features of friction stir welds in various materials. *TWI Rept.* 1999.
 14. Nandan R, DebRoy T, Bhadeshia HKDH. Recent advances in friction stir welding – Process, weldment structure and properties. *Progress in Materials Science.* 2008; 53:980-1023. <https://doi.org/10.1016/j.pmatsci.2008.05.001>
 15. Liu HJ, Fuji H. Mechanical properties of friction stir welded joints of 1050-H24 aluminium alloys. *Sci Technol Weld Joining.* 2003; 8(6):450-4. <https://doi.org/10.1179/136217103225005598>
 16. Hussain AK, Quadri SAP. Evaluation of parameters of friction stir welding for aluminium Aa6351 alloy. *International Journal of Engineering Science and Technology.* 2010; 2(10):5977-84.
 17. Rajakumar S, Muralidharan C, Balasubramanian V. Influence of friction stir welding process and tool parameters on strength properties of AA7075-T6 aluminium alloy joints. *Materials and Design.* 2011; 32:535-49. <https://doi.org/10.1016/j.matdes.2010.08.025>
 18. Nami H, Adgi H, Sharifitabar M, Shamabadi H. Microstructure, and mechanical properties of friction stir welded Al/Mg₂Si metal matrix cast composite. *Materials and Design.* 2011; 32:976-83. <https://doi.org/10.1016/j.matdes.2010.07.008>
 19. Karthikeyan L, Puviyarasan M, Sharath Kumar S, Balamugundan B. Experimental studies on friction stir welding of AA2011 and AA6063 aluminium alloys. *International Journal of Advanced Engineering Technology.* 2012; 3(4):144-5.
 20. Lee WonBae, Yeon YM, Jung SB. Effect of friction welding parameters on mechanical and metallurgical properties of aluminium alloy 5052-A36 steel joint. *Material Science Technology.* 2003; 19:1513. <https://doi.org/10.1179/026708303225001876>
 21. Chen YC, Liu H, Feng J. Friction stir welding characteristics of different heat-treated-state 2219 aluminium alloy plates. *Mater Science Engineering.* 2006; 420:21-5. <https://doi.org/10.1016/j.msea.2006.01.029>
 22. Kazuhiro N, Young Gon K, Masao U. Friction stir welding of Mg-Al-Zn alloys. *Trans JWRI.* 2002; 31:141-6.
 23. Ouyang JH, Kovacevic R. Material loss during Friction Stir Welding (FSW) of the same and dissimilar aluminium alloys. *Journal of Material Engineering Performance.* 2002; 11(1):51-63. <https://doi.org/10.1007/s11665-002-0008-0>
 24. Razal AR, Manisekar K, Balasubramanian V. Effect of axial force on microstructure and tensile properties of friction stir welded AZ61A magnesium alloy. *Transactions of Non-ferrous Metals Society of China.*

- 2011; 21:974-84. [https://doi.org/10.1016/S1003-6326\(11\)60809-1](https://doi.org/10.1016/S1003-6326(11)60809-1)
25. Karthikeyan M, Dawood AKS. influence of tool design on the mechanical properties and microstructure in friction stir welding of AA 6351 aluminium alloy. *An International Journal of Engineering Science and Technology*. 2012; 2(2).
26. Palanivel R, Mathews PK, Murugan N. Influences of tool pin profile on the mechanical and metallurgical properties of friction stir welding of dissimilar aluminium alloy. *International Journal of Engineering Science and Technology*. 2010; 2(6):2109-15.
27. Patel AKM, Ghetiya BND, Makvana CSJ. Influence of friction stir welding parameters on tensile strength of AA8011 aluminium. *Conference proceedings*.
28. Venkateswarlu D, Mandal NR, Mahapatra MM, Harsh SP. Tool design effects for FSW of AA7039. *Welding Journal*. 2013; 92.
29. Cavaliere P, Nobile R, Panella F, Squillace A. Mechanical microstructural behaviour of 2024-7075 aluminium *International Journal of Machine Tools and Manufacture*. 2006; 46:588-94. <https://doi.org/10.1016/j.ijmachtools.2005.07.010>
30. Kumar K, Kailas SV. The role of friction stir welding tool on the material flow and weld formation. *Material Science and Engineering*. 2008; 485:367-74. <https://doi.org/10.1016/j.msea.2007.08.013>
31. William JA. Friction stirs joining: Characteristic defects. *Advanced Materials Processing Center*. 2003.
32. Dilger DE. Apple slims down the iMac by 40% with 'friction stir welding' and ditching the disc drive. 2012. Retrieved from [Articles/12/10/24/apple-slims-down-imac-40-with-frictionstir-welding-ditching-the-disc-drive](http://www.appleinsider.com/articles/12/10/24/apple-slims-down-imac-40-with-frictionstir-welding-ditching-the-disc-drive) [Online] Available: <http://www.appleinsider.com/articles/12/10/24>.
33. Smith CB, Hinrichs JF, Ruehl PC. Friction stir and friction stir spot welding – Lean, Mean and Green. 2012. [Online] Available: www.frictionstirlink.com/Pub14AwssmcLeanMeanGreen.
34. Misra RS, Murray W, Mahoney. Friction stir welding and processing. 2007; 6-19.
35. Mehta M, Arora A, De A, Debroy T. Tool geometry for friction stir welding - Optimum shoulder diameter. 2011; 3. <https://doi.org/10.1007/s11661-011-0672-5>
36. Bisadi H, Tour M, Tayakoli A. The influence of process parameters on microstructure and mechanical properties of friction stir welded Al 5083 alloy lap joint. *American Journal of Materials Science*. 2011; 93-7. <https://doi.org/10.5923/j.materials.20110102.15>
37. Thomas WM, Nicholas ED, Needham JC, Murch MG, Smith PT, Dawes CJ. Friction-stir butt welding, GB Patent No. 9125978.8. *International Patent Application No. PCT/GB92/02203*; 1991.
38. Elangovan K, Balasubramanian V. Influences of pin profile and rotational speed of the tool on the formation of friction stir processing zone in AA2219 aluminium alloy. *Materials Science and Engineering*, 2007; 459:7-18. <https://doi.org/10.1016/j.msea.2006.12.124>
39. Kumbhar NT, Bhanumurthy K. Friction stir welding of Al 6061 alloy. *Asian J Exp Sci*. 2008; 22:63-74.
40. Zhang YN, Cao X, Larose S and Wanjara P. Review of tools for friction stir welding and processing. *Canadian Metallurgical Quarterly*. 2012; 51. <https://doi.org/10.1179/1879139512Y.0000000015>
41. Mishra RS, Ma ZY. Friction stir welding and processing. *Materials Science and Engineering*. 2005; 50:1-78. <https://doi.org/10.1016/j.mser.2005.07.001>
42. Kumar K, Kailas SV. The role of friction stir welding tool on the material flow and weld formation, *Materials Science and Engineering*. 2008; 367-74. <https://doi.org/10.1016/j.msea.2007.08.013>
43. Leonard AJ. Microstructure and ageing behaviour of FSW in Al alloys 2014A –T651 and 7075- T651, 2nd international symposium on FSW, Gothenburg, Sweden; 2000.
44. Soundarajan V, Yarrapareddy E, Kovacevic R. Investigation of the friction stir lap welding of aluminium alloys AA 5182 and AA 6022. *Journal of Material Engineering and Performance*. 2007; 16(4):477- 84. <https://doi.org/10.1007/s11665-007-9081-8>
45. HungTra T. Effect of weld parameters on mechanical properties of the friction stir welding aa6063-t5.
46. Karthikeyan P, Mahadevan K. Study on the weld quality of the friction stir welded Al 6063 plates using square and pentagonal profiled tools. *Journal of Applied Sciences*. 2012; 12(10):1026-31. <https://doi.org/10.3923/jas.2012.1026.1031>
47. Karthikeyan L, Puviyarasan M, Sharath SK, Balamugundan B. Experimental studies on friction stir welding of AA2011 and AA6063 aluminium

- alloys. *International Journal of Advanced Engineering Technology*. 2012; 3(4):144-5.
48. Pumchan W. The influences of friction stir welding on the microstructure and hardness of aluminium 6063 and 7075. *International Conference on Advanced Materials Engineering*; 2011. p. 15.
 49. Elangovan K, Balasubramanian V, Babu S. Predicting tensile strength of friction stir welded AA6061 aluminium alloy joints by a mathematical model. *Materials and Design*. 2009; 188-93. <https://doi.org/10.1016/j.matdes.2008.04.037>
 50. Rajakumar S, Muralidharan C, Balasubramanian V. Influence of friction stir welding process and tool parameters on strength properties of AA7075-T6 aluminium alloy joints. *Materials and Design*. 2011; 535-49. <https://doi.org/10.1016/j.matdes.2010.08.025>
 51. Shah LH, Othman NH, Gerlich A. Review of research progress on aluminium-magnesium dissimilar friction stir welding. *Sci Technol Weld Join*. 2018; 233(3):256-70. <https://doi.org/10.1080/13621718.2017.1370193>
 52. Shah IA, Khan R, Kolor SSR, Petru M, Badshah S, Ahmad S, Amjad M. Finite element analysis of the ballistic impact on auxetic sandwich composite human body armour. *Materials*. 2022; 15:2064. <https://doi.org/10.3390/ma15062064> PMID:35329516 PMCID: PMC8950186
 53. Shokravi H, Mohammadyan-Yasouj SE, Kolor SSR, Petru M, Heidarrezaei M. Effect of alumina additives on mechanical and fresh properties of self-compacting concrete: A review. *Processes*. 2021; 9:554. <https://doi.org/10.3390/pr9030554>
 54. Mazlan S, Yidris N, Kolor SSR, Petru M. Experimental and numerical analysis of fatigue life of aluminium Al 2024-T351 at elevated temperature. *Metals*. 2020; 10:1581. <https://doi.org/10.3390/met10121581>
 55. Koilraj M, Sundareswaran V, Vijayan S, Rao SK. Friction stir welding of dissimilar aluminium alloys AA2219 to AA5083– Optimization of process parameters using the Taguchi technique. *Mater. Des*. 2012; 42:1-7. <https://doi.org/10.1016/j.matdes.2012.02.016>
 56. Aamir M, Tolouei-Rad M, Giasin K, Vafadar A. Feasibility of tool configuration and the effect of tool material, and tool geometry in multi-hole simultaneous drilling of Al2024. *Int J Adv Manuf Technol*. 2020; 111:861-79. <https://doi.org/10.1007/s00170-020-06151-7>
 57. Sato YS, Urata M, Kokawa H, Ikeda K. Hall–Petch relationship in friction stir welds of equal channel angular-pressed aluminium alloys. *Mater Sci Eng*. 2003; 354:298-305. [https://doi.org/10.1016/S0921-5093\(03\)00008-X](https://doi.org/10.1016/S0921-5093(03)00008-X)
 58. Yong-Jai K, Seong-Beom S, Dong-Hwan P. Friction stir welding of 5052 aluminium alloy plates. *Trans Nonferrous Met Soc China*. 2009; 19:s23-7. [https://doi.org/10.1016/S1003-6326\(10\)60239-7](https://doi.org/10.1016/S1003-6326(10)60239-7)
 59. Yong-Jai K, Seong-Beom S, Dong-Hwan P. Friction stir welding of 5052 aluminium alloy plates. *Trans Nonferrous Met Soc China*. 2009; 19:s23-7. [https://doi.org/10.1016/S1003-6326\(10\)60239-7](https://doi.org/10.1016/S1003-6326(10)60239-7)
 60. Hosseinabadi OF, Khedmati MR. A review of the ultimate strength of aluminium structural elements and systems for marine applications. *Ocean Eng*. 2021; 232:109153. <https://doi.org/10.1016/j.oceaneng.2021.109153>
 61. Cheng Y, Hu Y, Xu J, Yu L, Huang T, Zhang H. Studies on microstructure and properties of TiB₂-Al₃Ti ceramic particles reinforced spray-formed 7055 aluminium alloy fusion welded joints. *J Mater Res Technol*. 2022; 19:1298-311. <https://doi.org/10.1016/j.jmrt.2022.05.116>
 62. Dawood H, Mohammed KS, Rahmat A, Uday M. Effect of small tool pin profiles on microstructures and mechanical properties of 6061 aluminium alloy by friction stir welding. *Trans Nonferrous Met Soc China*. 2015; 25:2856-65. [https://doi.org/10.1016/S1003-6326\(15\)63911-5](https://doi.org/10.1016/S1003-6326(15)63911-5)
 63. Msomi V, Mbana N, Mabuwa S. Microstructural analysis of the friction stir welded 1050-H14 and 5083-H111 aluminium alloys. *Mater Today Proc*. 2020; 26:189-92. <https://doi.org/10.1016/j.matpr.2019.10.038>
 64. Ali MH, Wadallah HM, Ibrahim MA, Alomar OA. Improving the microstructure and mechanical properties of aluminium alloy joints by adding SiC particles during the friction stir welding process. *Metallogr. Microstruct. Anal*. 2021; 10:302-13. <https://doi.org/10.1007/s13632-021-00743-9>
 65. Krishnaiah K, Shahabudeen P. *Applied design of experiments and Taguchi methods*. PHI Learning Pvt. Ltd.: Delhi, India; 2012.

Abbreviations

FSW	Friction Stir Welding
AA	Aluminium Association
TT	Taguchi Technique
TWI	The Welders Institution
Al	Aluminium
Cu	Copper
Mg	Magnesium
GMAW	Gas Metal Arc Welding
TIG	Tungsten Inert Gas Welding
MIG	Metal Inert Gas Welding
FSP	Friction Stir Processing
HAZ	Heat-Affected Zone
TMAZ	Thermo-Mechanically Affected Zone
SZ	Stir Zone
FSSW	Friction Stir Spot Welding
DOE	Design of Experiments
S/N	Signal-to-Noise Ratio
BM	Base Material
UTS	Ultimate Tensile Strength
RPM	Revolution Per Minute
θ	Tool Leaning Axis
RF	Ribbons Flashing
FZ	Fusion Zone
PcBN	Polycrystalline cubic Boron Nitrides
Ti	Titanium
C27H36CIN5O3	304L Stainless Steel
Mpa	Megapascal
ANNOVA	Analysis of Variance
ASTM E92	Standard Test Methods for Vickers Hardness and Knoop Hardness of Metallic Materials.
DNV	Det Norske Veritas